 ©2010 Kvantovaya Elektronika and Turpion Ltd

INTERACTION OF LASER RADIATION WITH MATTER. LASER PLASMA PACS numbers: 42.70.Ce; 42.79.Bh; 42.25.Bs; 61.80.Ba; 78.20.Ci
DOI: 10.1070/QE2010v040n09ABEH014309

Annealing of induced absorption in quartz glasses by ArF laser radiation

P.B. Sergeev, A.P. Sergeev

Abstract. **Annealing of individual bands of electron-beam-induced absorption (IA) in the region of 150 – 400 nm in KS-4V, KU-1, and Corning 7980 (ArF Grade) quartz glasses by ArF laser radiation is studied. It is shown that the photo-transformation of the IA spectra occurs mainly due to a significant decrease in the amplitudes of bands at $\lambda = 183.5$, 213, and 260 nm. The role played by interstitial oxygen, hydrogen, and chlorine in the formation and relaxation of glass defects is considered.**

Keywords: *quartz glasses, ArF laser radiation, photobleaching, induced absorption, colour centres, individual absorption bands.*

1. Introduction

The quartz glasses are basic materials for optics transmitting UV (including laser) radiation. The high-intensity UV radiation can considerably change their optical characteristics, which is one of the key problems in physics of quartz glasses.

At first, the gas-discharge excimer ArF lasers with a wavelength of 193 nm served only as a new tool for investigating defect formation in glasses [1 – 3]. However, the new opportunities opened for the use of their radiation in microelectronics for photolithography systems stimulated these investigations and focused them on the behaviour of particular glasses under irradiation typical for such systems [4 – 12].

It was shown that the 193-nm laser radiation forms in glasses the same defects as other ionisers [1 – 6]. In this case, the change in the optical characteristics of quartz glasses is mainly caused by the two-photon absorption of laser radiation, which lead to the appearance of E′ centres with an absorption band at 5.8 eV (214 nm) and non-bridging oxygen atoms (NOAs) absorbing at 4.8 eV (260 nm) [13 – 15]. The formation and stabilisation of this complementary pair of intrinsic defects in glasses after breaking the Si – O bond can occur if this bond was strained before ionisation. An increase in the radiation-induced yield of E′ centres in glass under mechanical stress was found in [16]. At the same time, the question of quantitative relation between the applied stress and the lifetime of the created defect pair remains open.

In glasses there are also other states, which can be precursors of E′ centres and NOAs. In particular, these are oxygen vacancies, or oxygen-deficient centres (ODCs) $\equiv$ Si – Si $\equiv$, and peroxide bridges (PBs) $\equiv$ Si – O – O – Si $\equiv$ [12], which are the simplest aggregates consisting of two E′ centres and NOAs. The maximum of the ODC absorption line lies at 7.6 eV (164 nm). It is assumed [4 – 6] that there is one more type of this defect, namely, unrelaxed oxygen vacancy ($\equiv$ Si$\cdots$Si $\equiv$) with the absorption line at 6.9 eV. Bond breaking in ODCs and PBs can produce E′ centres and NOAs, respectively.

Numerous experiments have shown that type III silica glasses with OH concentration of the order of 1000 ppm (wet glasses) have the highest resistance to long-term exposure to ArF laser radiation [4 – 6, 9 – 12]. These glasses have up to 10^{20}-cm^{-3} $\equiv$SiOH and $\equiv$SiH terminal bonds, which comprises a considerable portion of the total amount of regular Si – O bonds ($\sim 8.8 \times 10^{22}$ cm^{-3}). In wet glasses, the terminal bonds decrease the number of strained ones [5]. The localisation of electronic excitations or holes on terminal bonds leads to the detachment of hydrogen atoms and to the appearance of NOAs and E′ centres [17]. The subsequent relaxation of these defects occurs due to the capture of interstitial hydrogen atoms. It is these mechanisms of defect formation in vitreous SiO_2 under irradiation by an ArF laser that were proposed and simulated in [5 – 6, 9 – 12]. In these works, it was assumed that the linear absorption at 193 nm belongs to E′ centres.

The above models do not take into account the single-quantum stimulation of relaxation of defects formed due to the two-photon absorption. The contributions from these two processes are difficult to separate based only on the results of irradiation of the sample solely by laser radiation. The problem is easily solved in combined experiments, when an ioniser at first forms glass defects and then their photoresistance is studied. In particular, as we showed in [18], the radiation of a KrF laser reduces the electron-beam-induced absorption (IA) in pure silica glasses approximately by a factor of two. Previously, it was reported about quenching of the induced absorption in glasses under VUV irradiation by mercury lamps [13, p. 126] and under visible laser radiation [19], which proves that the accelerated relaxation of IA under action of laser radiation must be taken into account. It is also important to study these processes in detail under irradiation by lasers with $\lambda =$ 193 nm.

P.B. Sergeev, A.P. Sergeev P.N. Lebedev Physics Institute, Russian Academy of Sciences, Leninsky prosp. 53, 119991 Moscow, Russia; e:mail: psergeev@sci.lebedev.ru, sergandy@mail.ru

Received 11 March 2010; revision received 10 June 2010
Kvantovaya Elektronika **40** (9) 804 – 810 (2010)
Translated by M.N. Basieva

Analysing the results of [18], one can see that the radiation of KrF lasers with $\lambda = 248$ nm (5 eV) is absorbed both by the E′ centres and NOAs. It is still unclear the excitation of which of these centres due to the absorption of a photon accelerates their relaxation. It can be clarified by experiments with the ArF laser radiation, which is not absorbed by NOAs and absorbed by E′ centres. The radiation with $\lambda = 193$ nm can also be absorbed by other glass defects mentioned above. The aim of this work is to study the effect of the ArF laser radiation on defects formed by an electron beam (EB) in quartz glasses KS-4V, KU-1, and Corning 7980 (ArF Grade) (hereinafter C8). These glasses, which are widely used in UV optics, contain pairwise similar and different amounts of the main (Cl and OH) technological impurities. The KU-1 and C8 glasses have approximately identical amounts of OH (~ 1000 ppm) but strongly different amounts of chlorine, 200 and 20 ppm, respectively. The C8 and KS-4V glasses contain approximately the same amount of chlorine, but the concentration of OH in KS-4V is ~ 0.1 ppm. Comparing the results of investigations of these glasses, we can clarify the role played by the technological impurities in the physical processes occurring in their matrices under action of different radiations.

2. Experimental technique

The experiments on the long-term stability of the 3–4-mm-thick KS-4V, KU-4, and C8 quartz glass samples irradiated by 280-keV, 80-ns EB pulses were described in detail in [18, 20, 21]. The induced absorption of all the samples saturated with increasing the EB fluence. Some of these samples were then used in the experiments on annealing of IA by KrF laser radiation [18], after which they were additionally exposed to an electron beam on an ELA setup according to the standard technique. The samples were irradiated from the same face as before in the same regime [20, 21] with the EB fluence of about 2 J cm^{-2} per pulse. The additional fluence was 1 kJ cm^{-2}, and the overall fluence including the previous irradiation was 5.1 kJ cm^{-2} for KS-4V, 19.7 kJ cm^{-2} for KU-1, and 7.4 kJ cm^{-2} for C8.

Then, the samples were kept for more than two years in dark at a temperature of about 0 °C. Their transmission spectra $T(\lambda)$ were measured on an VMR-2 monochromator in the region of 150–240 nm and on a Spectronics Genesys-2 spectrophotometer in the region of 200–1000 nm. The numerical tables of the data on the dependence $T(\lambda)$ with the steps of 3 nm at $\lambda > 200$ and 2.5 nm at $\lambda < 200$ nm were used to plot the optical density dependences $D(\lambda) = \ln(T_0/T)$. Here, T_0 is the initial transmittance of the sample at the corresponding wavelength λ. In our opinion, the additional EB irradiation of the samples and their long-term storage lead the samples to the same state in which they were before the experiments with KrF laser radiation.

We irradiated the samples by an ArF laser on the ELA setup [22], which, in these experiments, generated pulses with an interval of 3–4 min. The ArF laser pulse duration was 60 ns. The laser pulse energy density on the samples was ~ 0.2 J cm^{-2}. In the process of laser irradiation, the transmittance of the samples at $\lambda = 193$ nm was determined in each pulse by measuring the incident and transmitted laser radiation energy with calorimeters. The $T(\lambda)$ spectra were measured before and several days after the laser irradiation.

3. Experimental results

Figure 1 shows the transmittance of a KU-1 sample at $\lambda = 193$ nm versus the ArF laser pulse number n_p. One can see that T increases from 54 % to 70 % after 60 pulses and then almost does not change under further irradiation. The transmittance of other quartz samples demonstrated almost the same behaviour. The $T(\lambda)$ spectra of these samples in this new quasi-stationary state are shown in Fig. 2 together with the spectra before irradiation. These spectra demonstrate that the ArF laser radiation with an intensity of about 3 MW cm^{-2} anneals the induced absorption in quartz glasses.

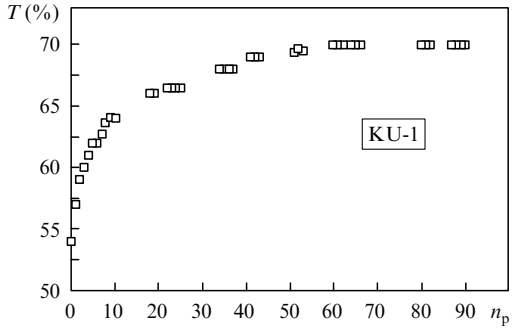

Figure 1. Dependence of the transmittance of a KU-1 glass sample at 193 nm on the ArF laser pulse number.

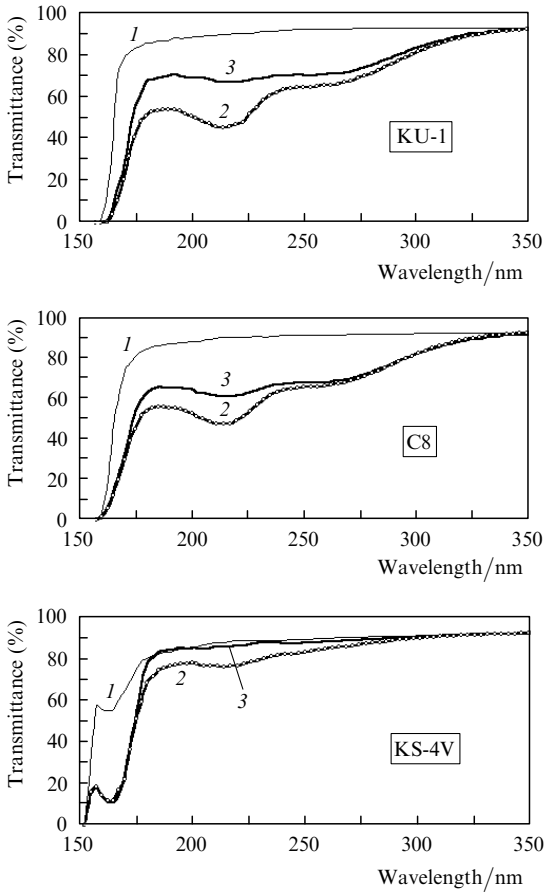

Figure 2. Transmittance spectra of the studied glass samples before EB irradiation (*1*), as well as before (*2*) and after irradiation by an ArF laser.

This effect can be easier analysed using the optical density spectra (Fig. 3) for the same samples. In addition to the $D(\lambda)$ spectra before and after irradiation by the ArF laser, Fig. 3 also shows their difference. After irradiation, the densities D at $\lambda = 193$ nm decrease from 0.49 to 0.22 for KU-1, from 0.46 to 0.29 for C8, and from 0.089 to -0.007 for KS-4V. The negative D for KS-4V means that the entire thickness of this sample becomes more transparent than in the initial state before EB irradiation and even more so than before laser irradiation. Such bleaching of quartz glasses under irradiation by an ArF laser was previously observed in [7].

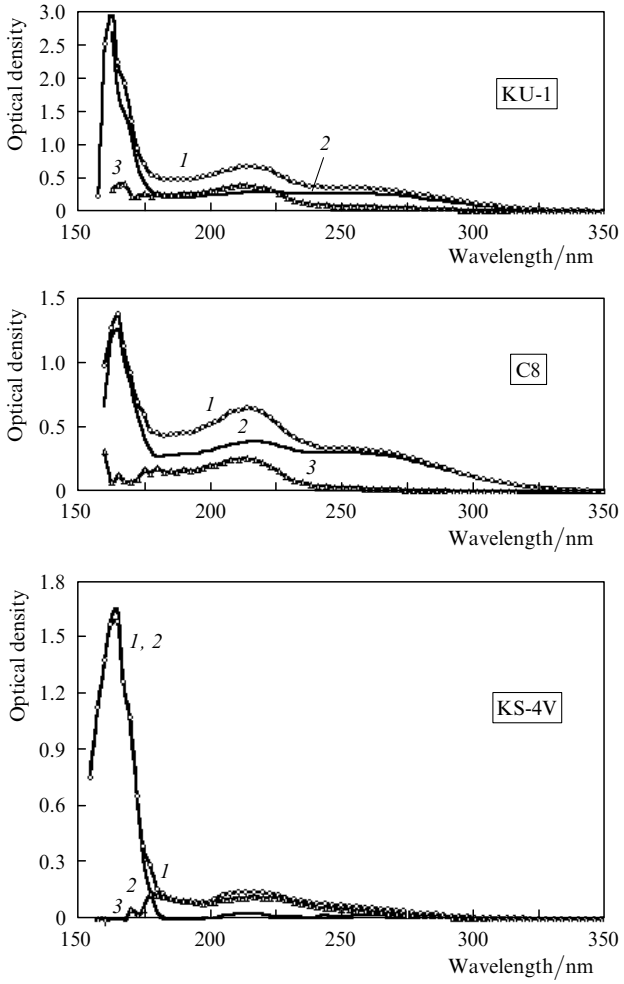

Figure 3. Spectra of the optical density of the studied glass samples before (*1*) and after (*2*) irradiation by an ArF laser and their difference (*3*).

To quantitatively analyse the photobleaching of induced absorption in glasses, we decomposed all their spectra $D(\lambda)$ (Fig. 3) into individual bands by a method used by us previously to analyse the IA spectra in MgF_2 [23]. Examples of this decomposition for the C8 sample before and after irradiation by an ArF laser, as well as the decomposition of the difference spectrum, are shown in Fig. 4. All the used individual bands were described by the Gaussian energy profiles and, depending on λ, had the shape

$$L(\lambda_{mi}) = A_i \exp\left[-\ln 2\left(\frac{E_{mi}}{\Delta E_i}\right)^2\left(\frac{\lambda_{mi}-\lambda}{\lambda}\right)^2\right]. \qquad (1)$$

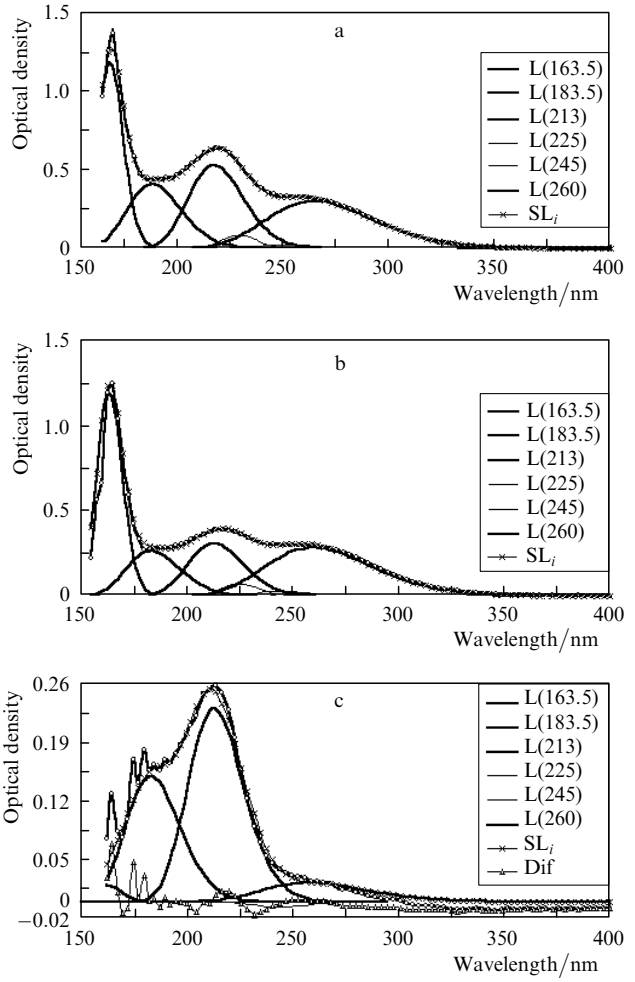

Figure 4. Decomposition of the $D(\lambda)$ spectra of the C8 sample on individual bands: spectrum before laser irradiation (line with circles), calculated spectrum (SL_i), and individual bands in this spectrum [$L(\lambda_{mi})$] (a); the same after irradiation of the sample by an ArF laser (b); and the same for the difference spectrum (Dif denotes the difference between the experimental and calculated spectra) (c).

Here, A_i is the amplitude coefficient of the band in the corresponding spectrum, E_{mi} is the position of the band maximum at the energy scale, ΔE_i is band half-width, and λ_{mi} is the wavelength of the band peak. The calculated spectra depicted by SL_i in Fig. 4 represent the sums of contributions from all the individual bands.

Table 1 lists the characteristics of the individual bands used in the decomposition of all the $D(\lambda)$ spectra of the studied glasses. The procedure of this decomposition consisted in minimisation of the difference between the experimental and calculated spectra $D(\lambda)$ by selecting corresponding parameters A_i, E_{mi} (and, hence, λ_{mi}), and ΔE_i. This difference in our calculations did not exceed 0.01,

Table 1. Characteristics of individual absorption bands of quartz glasses.

Band	λ_{mi}/nm	E_{mi}/eV	ΔE_i/eV	Absorbing centre
1	260	4.8	0.54	NOA
2	245	5.1	0.27	ODC(2)?
3	225	5.54	0.25	?
4	213	5.86	0.42	E′ centre
5	183.5	6.8	0.55	?
6	163.5	7.63	0.33	ODC

which corresponds to the accuracy of the experimental D. As a rule, more significant discrepancies appeared in the form of independent bands, which were observed in different spectra and for different samples. In Fig. 4, these low-intensity bands are clearly seen in the curve corresponding to the difference between the experimental and calculated D, which is depicted as Dif. The possible nature of these bands will be discussed below.

At the first stage of the IA spectrum decomposition, we used the characteristics of individual bands from [7, 13–15]. The following multiple refinements of decomposition curves by varying the corresponding parameters yielded the results (Table 1) almost completely coinciding with experimental. They were obtained based on the above-described processing of about hundred of EP-induced absorption spectra [20, 21] and their modifications after irradiation by KrF [18] and ArF lasers in KU-1, KS-4V, and C8 quartz glasses.

The decomposition of spectra into individual bands allows one to describe them by a set of A_i coefficients equal to the product of the absorption cross section σ_{mi} at the wavelength λ_{mi} and the surface density N_{si} of the corresponding defects. The knowledge of N_{si} simplifies the interpretation of processes occurring in glasses. Table 2 presents the coefficients A_i obtained by decomposition of all the $D(\lambda)$ spectra shown in Fig. 3 into individual bands. In this table, the coefficients A_i for the $\Delta D(\lambda)$ spectra of corresponding samples must be equal to the difference between their values given above. The existing discrepancies are related to the accuracy of determination of these coefficients, which on average did not exceed 0.03.

In addition, Table 2 presents the characteristics of the spectra measured one hour and one month after the last shot from the electron gun in the process of their additional EB irradiation. Comparison of these spectra with the spectra 'before ArF' shows the degree of relaxation of the corresponding IA components for 2.3 years of storage.

4. Discussion of results

To analyse the physical processes of IA annealing by ArF laser radiation, it is necessary to know which defects are responsible for the induced absorption. The nature of the bands in Table 1 is known with different degrees of reliability. In particular, the first band parameters well coincide with the data on NOAs [13–15]. This band may hide the weaker bands of interstitial O_3 molecules [14], as well as of the bridging complexes (OCl), (O_2Cl), (H), and (Cl_2) absorbing near 260 nm [24]. These bands were sometimes observed in our spectra near the sensitivity limit.

A similar situation is with the fourth band, which we assign to the E′ centres [13–15]. This band can also mask other components, most of which belong to the three- of two-co-ordinated silicon atoms in different charge states and with different nearest environment [24]. When decomposing the spectra, we in some cases had to change the wavelength of this band maximum, but no stronger than by 1 nm, which can reflect the variations in the composition of centres absorbing in this region.

The relation of the six band to the ground state of ODCs is also convincingly proved [13–15], but the rather large spread of its key parameters points to the presence of other absorbers in this spectral region. In particular, the position of its maximum varied within 163.5 ± 1 nm and ΔE_6 changed within the range of 0.33 ± 0.03 eV. In addition, the Dif spectra in Fig. 4c clearly show narrow (~ 0.1 eV) bands peaked at 165, 175, and 180 nm. The same structure was observed in the KU-1 sample, but the intensity of the shortest-wavelength band at 167.5 nm in this case was approximately twofold higher, while the bands at 175 and 180 nm had the same intensity as for C8. The corresponding spectra for KS-4V glass had the bands peaked at 160, 170, and 177.5 nm with almost identical amplitudes. The existence of these bands was predicted in [24]. They are attributed to peroxy radicals (160 nm), complexes $=SiH_2$ (175 nm), and complexes $=SiCl_2$ (180 nm). The intensities of these bands are low, at the level of 1 %–5 % of the intensity of the dominant ODC band, but, nevertheless, they can affect its characteristics.

In the region of 7.5 eV, one also observes the absorption tails of $\equiv SiOH$ [25–27] and interstitial O_2 [28, 29] and H_2O [29] molecules. Their concentrations depend on the glass history, especially if they were exposed to ionising or laser radiation [30], which may manifest itself in variations in the characteristics of the six absorption band. These variations were also observed in [31].

The second and third bands were revealed by us when analysing the results on the induced absorption in glasses, which was easily annealed by KrF laser radiation [18]. We managed to describe the difference spectra using these two bands. Their intensities in KS-4V are almost identical, but

Table 2. Coefficients A_i in the spectra of KU-1, C8, and KS-4V glasses one hour, one month, and 2.3 years ('before ArF') after EB irradiation, as well as after irradiation by an ArF laser; $\Delta D(\lambda)$ is the difference between the $D(\lambda)$ spectra before and after laser irradiation.

Glass	Irradiation conditions	A_1/260 nm	A_2/245 nm	A_3/225 nm	A_4/213 nm	A_5/183.5 nm	A_6/163 nm
KU-1	1 h	0.56	0.01	0.09	1.16	0.85	–
	before ArF	0.33	0.03	0.08	0.57	0.47	2.7
	after ArF	0.26	0.02	0.06	0.21	0.22	2.4
	$\Delta D(\lambda)$	0.08	−0.02	−0.02	0.38	0.24	0.33
C8	1 h	0.4	0.05	0.12	0.75	0.51	–
	1 month	0.35	0.03	0.12	0.63	0.52	1.3
	before ArF	0.3	0.03	0.11	0.59	0.41	1.25
	after ArF	0.28	0.03	0.07	0.31	0.26	1.2
	$\Delta D(\lambda)$	0.02	−0.01	0	0.23	0.15	0.02
KS-4V	1 h	0.06	0.04	0.04	0.22	0.15	–
	before ArF	0.04	0.03	0.03	0.12	0.08	1.57
	after ArF	0.02	0	0	0.03	−0.01	1.67
	$\Delta D(\lambda)$	0.02	0.03	0.03	0.09	0.09	−0.09

the 225-nm band dominates in the spectra of wet glasses. The nature of these bands has been discussed for a long time [13], but is not yet completely clear [14, 15].

Concerning the band at 245 nm (5.1 eV), which is called ODC(2) [13–15], we should note the following: 2.3 years after additional EB irradiation, the intensities of this band became identical for all the samples, which can be seen from Table 2, lines 'before ArF'. At the same time, compared to the situation immediately after irradiation, this band intensity decreased in the case of KU-1 and slightly decreased C8 and KS-4V. The strange behaviour of this band in different glasses, as well as its small intensity and low photostability, can be explained, in our opinion, by its belonging to surface centres.

The behaviour of the weak third band at 225 nm (5.54 eV) also demonstrates many unusual features. Note that its intensity decreased for 2.3 years after the additional EB irradiation much weaker than the intensities of the first, fourth, and fifth bands, which points to a high chemical stability of this band. This is especially surprising in combination with the low photostability. We suppose that these properties can be inherent in nitrogen centres considered in [24].

The nature of the strong fifth band peaked at 183.5 nm (6.8 eV) is also unclear [5, 7, 14, 15, 32, 33]. Its intensity is close to the arithmetic mean between the intensities of NOAs and E′ centres, which testifies to their interrelation. All these centres have similar relaxation rates. Comparison of the intensities of bands in corresponding spectra from Table 2 shows the absence of strict correlation between them. Therefore, all these bands (at least their main components) belong to different defects, which refutes the suggestion [14, 15] that the bands at 260 and 183 nm belong to the same absorption centres.

The partial attribution of individual bands to known defects and the knowledge of their absorption cross sections in the maximum σ_{mi} allow one to determine only some surface defect densities N_i using the relation $N_i = A_i/\sigma_{mi}$. The values of σ_{mi} were taken from [14]: $\sigma_{m1} = 5.3\times 10^{-18}$ cm^2, $\sigma_{m4} = 2.5\times 10^{-17}$ cm^2, and $\sigma_{m6} = 7.5\times 10^{-17}$ cm^2. Therefore, Table 2 was transformed to Table 3, whose data will be consider below.

The first important fact in Table 3 is the difference between N_1 and N_4 for different glasses (see lines '1 hour' and 'before ArF'). Indeed, ionising radiation at first breaks the Si–O bonds in quartz glasses. In this case, the number of the primary E′ centres and NOAs must be identical. Due to a large irradiation duration, the primary defect pairs in process of relaxation can bind to mobile interstitial atoms and molecules, which will change their equality. A difference may also appear due to the defect formation as a result of detachment of atoms from terminal bonds. In wet glasses, the dominant complexes are ≡SiOH. The detachment of a hydrogen atom from them will form NOAs. Due to the diffusion of H, the inverse process will reduce this complex, but in a different place. This causes a considerable spatial separation of primary E′ centres and NOAs, which increases the number of long-lived centres. These reactions do not affect the total balance between N_1 and N_4, but, if the detached hydrogen atoms remain in interstitials due to some reasons, the number of NOAs will be larger.

Due to a strongly different content of OH in glasses, it is the reactions with hydrogen that determine the difference in the amount and ratio between the E′ centres and NOAs in C8 and KS-4V, which follows from Table 3. Since NOAs evidently dominate in C8 (as well as in KU-1), the content of ≡SiH defects, even if they exist, is low. In the opposite case, the detachment of hydrogen from this defect and the following more probable binding of H to a NOA would form mainly the E′ centres.

Chlorine also forms terminal bonds of the ≡SiCl and ≡SiOCl types. Its binding energy in these bonds is almost the same [14], and, hence, the number of E′ centres and NOAs formed due to the Cl detachment should be approximately identical (as well as the number of inverse reactions). In this case, due to diffusion, Cl (similar to H) will be bound in another place, thus causing spatial separation and, hence, stabilisation of the primary E′ centres and NOAs. Obviously, this is a universal mechanism of reduction of radiation resistance of quartz glasses with hydrogen impurities, as well as of alkaline and halide atoms closing the terminal bonds.

The data on A_6 and N_6 in Tables 2 and 3 are also worthy of notice. The appearance of ODCs in the regular glass lattice regions must be accompanied by the release of oxygen atoms into interstitials. This may occur due to their knocking-out by electrons with energies exceeding 110 keV [13, p. 110]. This mechanism is universal and should yield almost identical amounts of ODCs and interstitial oxygen in all glasses under similar irradiation conditions. The twofold

Table 3. Values of N_i for the corresponding spectra of glass samples from Table 2.

Glass	Irradiation conditions	$N_1/10^{16}$ cm^{-2}	A_2/245 nm	A_3/225 nm	$N_4/10^{16}$ cm^{-2}	A_5/ 183.5 nm	$N_6/10^{16}$ cm^{-2}
KU-1	1 h	10.6	0.01	0.09	4.6	0.85	$\geqslant 3.6$
	before ArF	6.2	0.03	0.08	2.3	0.47	3.6
	after ArF	4.9	0.02	0.06	0.8	0.22	3.2
	$\Delta D(\lambda)$	1.5	−0.02	−0.02	1.5	0.24	0.4
C8	1 h	7.5	0.05	0.12	3	0.51	$\geqslant 1.7$
	1 month	6.6	0.03	0.12	2.5	0.52	1.7
	before ArF	5.7	0.03	0.11	2.4	0.41	1.67
	after ArF	5.3	0.03	0.07	1.2	0.26	1.6
	$\Delta D(\lambda)$	0.4	−0.01	0	0.9	0.15	0.03
KS-4V	1 h	1.13	0.04	0.04	0.88	0.15	$\geqslant 2.1$
	before ArF	0.75	0.03	0.03	0.48	0.08	2.1
	after ArF	0.38	0	0	0.12	−0.01	2.2
	$\Delta D(\lambda)$	0.38	0.03	0.03	0.36	0.09	−0.1

higher N_6 for KU-1 is explained by the higher EB fluence for this sample.

We admit the possibility of other mechanisms of interstitial oxygen formation. This is evidenced by the results of work [34], in which interstitial oxygen was observed in glasses under X-ray irradiation with a maximum energy of 45 keV, which is obviously insufficient for realisation of impact mechanisms. However, these questions require additional consideration. Of importance for our study is the mere fact that interstitial oxygen atoms appear under EB irradiation of glasses. It should also be noted that a small (of the order of 5×10^{15} cm^{-3}) amount of O_2 can accumulate in interstitials of glasses due to its diffusion from air [28].

The interstitial oxygen and chlorine appeared in glasses under EB irradiation can bind the hydrogen atoms released into interstitials and thus form molecules and radicals, in particular, H_2O, HCl, and OH. The number of hydrogen atoms 'stuck' to these molecules determines the excess of NOAs with respect to E′ centres. The binding of oxygen by the E′ centres with formation of NOAs may also change the ratio between these defects.

In KS-4V dry glasses, O and Cl atoms should form O_2, Cl_2, OCl, and OCl_2 molecules, which was observed in [34]. The slow relaxation of NOAs and E′ centres during ionising irradiation and after it is substantially determined by their interactions with the interstitial molecules. As follows from Table 3, the interaction of the primary defects with interstitial oxygen and chlorine for more than two years changes the N_1/N_4 ratio for KS-4V approximately from 1.3 to 1.6. This ratio in wet glasses is close to 2.5. This difference is caused by the binding of interstitial hydrogen to oxygen followed by a more probable reaction of OH or H_2O with E′ centres.

In 2.3 years after EB irradiation of glass samples, the interstitials can still contain oxygen, chlorine, water, and HCl molecules and OH and OCl radicals covalently bound to oxygen atoms from regular glass lattice regions [14]. As one can see from Fig. 4, the ArF laser wavelength falls within the absorption band at $\lambda = 183$ nm and the absorption band of E′ centres. The ArF laser radiation can also be absorbed by O_2, H_2O, and HCl molecules [28, 29, 35], but their absorption cross sections at $\lambda = 193$ nm are small. Therefore, in the case of low-intensity ArF laser radiation, the observed fast bleaching of IA in glasses is caused mainly by the processes occurring upon absorption of photons by glass defects.

This is also proved by the results presented in Tables 2 and 3. The 183.5-nm band intensity in wet glasses decreased approximately twofold, while this band in KS-4V faded completely. The number of E′ centres decreased approximately by a factor of 3 in KU-1, by a factor of two in C8, and by a factor of 4 in KS-4V. The number of NOAs in arbitrary units decreased less steeply: by approximately 20 % in KU-1, 7 % in C8, and approximately 50 % in KS-4V. At the same time, it should be noted that the decrease in the number of NOAs and E′ centres [line $\Delta D(\lambda)$ in Table 3] is almost the same for KU-1 and KS-4V. Based on this similarity, we can conclude that the laser irradiation into the absorption band of E′ centres leads to annihilation of the long-lived but close defect pairs of E′ centres and NOAs. However, this process may also involve defects with the absorption band at $\lambda = 183$ nm, which is shown by experiments on IA annealing by KrF laser radiation [18], whose wavelength does not fall into the absorption band at 183 nm, but which, nevertheless, decreases this band intensity approximately twofold [36]. To date, the absence of exact knowledge of this band nature does not allow one to study the processes of laser annealing of induced absorption in quartz glasses in more detail.

5. Conclusions

The annealing of EB-induced absorption in modern high-purity quartz glasses KS-4V, Corning 7980 (C8), and KU-1 by ArF laser radiation was studied. All the IA spectra of the studied glass samples were decomposed into six individual bands, whose amplitude variations under laser irradiation were then analysed. It is shown that the ArF laser radiation decreases the intensities of almost all the individual bands. In particular, in KS-4V glass, the 245-, 225-, and 183-nm bands fade completely, while the number of E′ centres and NOAs decreases by a factor of four and two, respectively. The intensities of the IA bands at 260, 245, 225, and 163 nm in wet KU-1 and Corning 7980 glasses decrease insignificantly, within 10 % – 20 %, while the intensities of the bands at 213 and 183 nm decrease approximately twofold.

The analysis of the experimental data shows that the induced absorption of the studied quartz glasses is reduced under action of both 193- and 248-nm laser radiation mainly due to the stimulated relaxation of close defect pairs of E′ centres and NOAs, as well as of the centres absorbing at 183 nm, upon photoexcitation of any of them. An important role in the formation and relaxation of defects in glasses is also played by interstitial oxygen, nitrogen, and chlorine atoms and their compounds formed under irradiation.

In our opinion, the presented experimental results and their analysis will be useful for designers of high-power UV and VUV lasers, as well as for quartz glass manufacturers and physicists studying the problems of radiation defect formation in these glasses.

Acknowledgements. The authors thank V.M. Reiterov, D.B. Stavrovskii, and G.G. Dubrovskaya for their help in spectral measurements.

References

1. Arai K. et al. *Appl. Phys. Lett.*, **53**, 1891 (1988).
2. Tsai T.E., Griscom D.L., Friebele E.J. *Phys. Rev. Lett.*, **61**, 444 (1988).
3. Tsai T.E., Griscom D.L. *Phys. Rev. Lett.*, **67**, 2517 (1991).
4. Rothschild M., Sedlacek J.H.C. *Proc. SPIE Int. Soc. Opt. Eng.*, **1848**, 537 (1992).
5. Kuzuu N. *Proc. SPIE Int. Soc. Opt. Eng.*, **2714**, 41 (1996).
6. Kuzuu N. *Proc. SPIE Int. Soc. Opt. Eng.*, **2714**, 71 (1996).
7. Saito K. et al. *J. Appl. Phys.*, **86**, 3497 (1999).
8. Kuhnlenz F. et al. *J. Non-Cryst. Sol.*, **278**, 115 (2000).
9. Shimbo M. et al. *J. Appl. Phys.*, **88**, 6052 (2000).
10. Natura U. et al. *Proc. SPIE Int. Soc. Opt. Eng.*, **5273**, 155 (2004).
11. Muhlig Ch., Triebel W., Kufert S. *J. Non-Cryst. Sol.*, **353**, 542 (2007).
12. Muhlig Ch., Stafast H., Triebel W. *J. Non-Cryst. Sol.*, **354**, 25 (2008).
13. Silin' A.P., Trukhin A.N. *Tochechnye defecty i elementarnye vozbuzhdeniya v kristallicheskom i stekloobraznom SiO_2* (Point Defects and Elementary Excitations in Crystalline and Vitreous SiO_2) (Riga: Zinatne, 1985).

14. Skuja L., Hosono H., Hirano M. *Proc. SPIE Int. Soc. Opt. Eng.*, **4347**, 155 (2001).
15. Skuja L. et al. *Phys. Stat. Sol. (C)*, **2**, 15 (2005).
16. Pavlychev I.K., Bobyshev A.A., Butyagin P.Yu. *Khim. Fiz.*, **6**, 188 (1987).
17. Arbuzov V.I. *Osnovy radiazionnogo opticheskogo materialovedeniya. Uchebnoe posobie* (Fundamentals of Radiation Optical Material Science. School Book) (St. Petersburg: SPbGUITMO, 2008).
18. Sergeev P.B., Sergeev A.P., Zvorykin V.D. *Kvantovaya Elektron.*, **37** (8), 711 (2007) [*Quantum Electron.*, **37** (8), 711 (2007)].
19. Dianov E.M. et al. *Kvantovaya Elektron.*, **11** (12), 2480 (1984) [*Sov. J. Quantum Electron.*, **14** (12), 1637 (1984)].
20. Sergeev P.B. et al. *Opt. Zh.*, **71**, 93 (2004).
21. Sergeev P.B., Sergeev A.P., Zvorykin V.D. *Kvantovaya Elektron.*, **37** (8), 706 (2007) [*Quantum Electron.*, **37** (8), 706 (2007)].
22. Sergeev P.B. *J. Sov. Laser Research*, **14** (4), 237 (1993).
23. Sergeev P.B., Sergeev A.P. *Kvantovaya Elektron.*, **38** (3), 251 (2008) [*Quantum Electron.*, **38** (3), 251 (2008)].
24. Dianov E.M., Sokolov V.O., Sulimov V.B. *Trudy IOFAN*, **23**, 122 (1990).
25. Morimoto Y., Nozawa S., Hosono H. *Phys. Rev. B*, **59**, 4066 (1999).
26. Kajihara K. et al. *J. Non-Cryst. Sol.*, **352**, 2307 (2006).
27. Vella E., Boscaino R., Navarra G. *Phys. Rev. B*, **77**, 165203 (2008).
28. Kajihara K. et al. *J. Appl. Phys.*, **98**, 013527 (2005).
29. Kajihara K. et al. *J. Non-Cryst. Sol.*, **352**, 2303 (2006).
30. Kajihara K. et al. *Phys. Stat. Sol. (C)*, **2**, 314 (2005).
31. Cannas M. et al. *J. Non-Cryst. Sol.*, **280**, 188 (2001).
32. Kajihara K. et al. *Nucl. Instr. Meth. Phys. Research B*, **218**, 323 (2004).
33. Larionov Yu.V., Sokolov V.O., Plotnichenko V.G. *Kvantovaya Elektron.*, **37** (6), 575 (2007) [*Quantum Electron.*, **37** (6), 575 (2007)].
34. Zhang L., Mashkov V.A., Leisure R.G. *Phys. Rev. B*, **53**, 7182-71 (1996).
35. Okabe H. *Photochemistry of Small Molecules* (New York: John Wiley & Sons, 1978; Moscow: Mir, 1981).
36. Sergeev P.B., Sergeev A.P. *Tesisy dokladov XXIV S'ezda po spectroscopii* (Proceedings of the XXIV Conference on Spectroscopy) (Moscow, Troitsk, 2010) Vol. 1, p. 222.